ADVANCING EARTH AND SPACE SCIENCE

JGR Biogeosciences

RESEARCH ARTICLE
10.1029/2021JG006396

Key Points:

- Collapse-scar bog ages at our sites were not related to feature size and may have been more influenced by local factors
- We found smaller losses of C with permafrost thaw than other studies from Interior Alaska
- The timing of permafrost aggradation relative to peat accumulation is an important factor in determining how much C is lost with thaw

Supporting Information:

Supporting Information may be found in the online version of this article.

Correspondence to:

K. L. Manies,
kmanies@usgs.gov

Citation:

Manies, K. L., Jones, M. C., Waldrop, M. P., Leewis, M.-C., Fuller, C., Cornman, R. S., & Hoefke, K. (2021). Influence of permafrost type and site history on losses of permafrost carbon after thaw. *Journal of Geophysical Research: Biogeosciences*, *126*, e2021JG006396. https://doi.org/10.1029/2021JG006396

Received 13 APR 2021
Accepted 8 OCT 2021

Author Contributions:

Conceptualization: Miriam C. Jones, Mark P. Waldrop
Data curation: Miriam C. Jones, Mary-Cathrine Leewis, Christopher Fuller, Kristen Hoefke
Formal analysis: Mary-Cathrine Leewis, Robert S. Cornman
Methodology: Mary-Cathrine Leewis, Christopher Fuller
Project Administration: Mark P. Waldrop
Validation: Christopher Fuller
Writing – original draft: Miriam C. Jones
Writing – review & editing: Miriam C. Jones, Mark P. Waldrop, Mary-Cathrine Leewis, Christopher Fuller, Robert S. Cornman, Kristen Hoefke

Influence of Permafrost Type and Site History on Losses of Permafrost Carbon After Thaw

Kristen L. Manies[1], Miriam C. Jones[2], Mark P. Waldrop[1], Mary-Cathrine Leewis[1,3], Christopher Fuller[4], Robert S. Cornman[5], and Kristen Hoefke[5]

[1]Geology, Minerals, Energy, and Geophysics Science Center, U.S. Geological Survey, Menlo Park, CA, USA, [2]Florence Bascom Geoscience Center, U.S. Geological Survey, Reston, VA, USA, [3]Now at Agriculture and Agri-Food Canada, Quebec, QC, Canada, [4]Water Science Center, U.S. Geological Survey, Menlo Park, CA, USA, [5]Fort Collins Science Center, U.S. Geological Survey, Fort Collins, CO, USA

Abstract We quantified permafrost peat plateau and post-thaw carbon (C) stocks across a chronosequence in Interior Alaska to evaluate the amount of C lost with thaw. Macrofossil reconstructions revealed three stratigraphic layers of peat: (a) a base layer of fen/marsh peat, (b) peat from a forested peat plateau (with permafrost), and (c) collapse-scar bog peat (at sites where permafrost thaw has occurred). Radiocarbon dating revealed that peat initiated within the last 2,500 years and that permafrost aggraded during the Little Ice Age (ca. 250–575 years ago) and degraded within the last several decades. The timing of permafrost thaw within each feature was not related to thaw bog size. Their rate of expansion may be more influenced by local factors, such as ground ice content and subsurface water inputs. We found C losses due to thaw over the past century were up to 46% of the C available, but the absolute amount of C lost (kg m^{-2}) was over 50% lower than losses previously described in other Alaskan peatland chronosequences. We hypothesize that this difference stems from the process by which permafrost aggraded, with sites that formed permafrost epigenetically (significantly later than most peat accumulation) experiencing less absolute C loss with thaw than sites that formed syngenetically (simultaneously with peat accumulation). Epigenetic peat from our site had lower C:N ratios as compared to Alaskan sites that have syngenetic peat. This difference could help predict the magnitude of C loss with thaw across a range or permafrost types and histories.

Plain Language Summary We quantified peat carbon at a permafrost peatland in Alaska to see how much carbon was lost from the peat when permafrost, or frozen soil, thawed and that area became a collapse-scar bog. We found that size of the bog was unrelated to its age. Factors, such as the amount of ice in the soil and water entering the bogs from the surrounding forests, may have been more important in determining their growth. Carbon losses at our site were lower than carbon losses found from other Alaskan sites. We compared our results to other studies, some which had small losses of carbon due to thaw, others which found large losses. We found that factors related to time (i.e., age since peat initiation, number of years the site had permafrost) are important but do not fully explain these different results. However, when we include how permafrost formed we see a trend: sites where permafrost formed after peat (epigenetic permafrost) had smaller carbon losses than sites where permafrost and peats formed at the same time (syngenetic permafrost). Determining permafrost type can be difficult; instead scientists can use C:N ratios to determine if their samples resemble peat formed by epigenetic versus syngenetic permafrost.

1. Introduction

Northern peatlands play an important role in the global carbon (C) budget and are estimated to store 415 Pg of C (±150 Pg C; Hugelius et al., 2020), which represents ~20% of the global soil C stock (Jackson et al., 2017). Close to half of this C has been protected from decomposition by permafrost, substrate that has remained frozen for at least two consecutive years (Rodenhizer et al., 2020). Permafrost in northern peatlands reached its maximum extent around 1700 Common Era (CE), with the highest rates of aggradation between 1,200 and 1,950 CE (Treat & Jones, 2018). Much of this permafrost is found in the discontinuous zone, where areas of permafrost are found adjacent to areas of unfrozen soil. In the discontinuous zone, the majority of which resides above 60°N (Brown et al., 1997), the presence of permafrost depends on the area's climate (both past and present) as well as local factors, such as vegetation, aspect, thickness of organic soil horizons, and texture of the mineral soil (Shur & Jorgenson, 2007). Permafrost can form either after the accumulation of peat/sediments (epigenetic permafrost) or concurrent with peat/sediment deposition (syngenetic permafrost). Between 2.20 and 3.95×10^6 km^2 of the northern hemisphere is estimated to have discontinuous permafrost (Obu et al., 2019; Zhang et al., 2000).

Permafrost peatlands within the discontinuous zone are often associated with forested peat plateaus (Gibson et al., 2019). Typically, these ecosystems are vegetated with black spruce (*Picea mariana*) trees and ericaceous shrubs, such as Labrador Tea (*Rhododendron groenlandicum*), with a ground cover of feather mosses and *Sphagnum* spp. The underlying organic soil, or peat, can be up to 6 m thick (Gibson et al., 2019). The uppermost peat, known as the active layer, undergoes seasonal freezing and thawing and is usually 0.3–0.7 m thick, with permafrost found below (Shur et al., 2011). Microbial decomposition of organic matter (OM) in this frozen soil is dramatically reduced compared to unfrozen soils, thereby stabilizing a large pool of potentially labile C (Harden et al., 2012; Leewis et al., 2020). Once thawed, this reserve of C is available for more rapid decomposition, which results in losses of C from the soil, much of which is lost to the atmosphere.

Over the past few decades, air temperatures within the northern high latitudes have warmed at a faster rate than other locations around the globe (Oliva & Fritz, 2018). These changes have increased soil temperatures (Jungqvist et al., 2014), growing-season length (Euskirchen et al., 2009), and both fire frequency and intensity (Turetsky et al., 2011), all of which impact permafrost stability and C storage within these landscapes. In well drained sites, post-thaw conditions usually result in water draining from the soil, resulting in oxic soil conditions (Estop-Aragonés, Cooper, et al., 2018). However, permafrost thaw in lowlands often results in subsidence and inundation, changing the ecosystem from a relatively dry, forested peat plateau to bogs or fens with a near-surface water table (Schuur et al., 2015), resulting in a soil profile that is primarily anaerobic or microaerobic.

In lowlands, transitioning from a forested peat plateau to an inundated wetland impacts C cycling in several ways. First, this transition results in wholesale changes in vegetation; trees die as their roots become inundated with ground subsidence, resulting in a shift in dominance to inundation-tolerant *Sphagnum* and/or *Carex* spp. (Finger et al., 2016). Increases in the amount of *Sphagnum* impacts C accumulation rates (Thormann et al., 1999), as *Sphagnum* is known to reduce decomposition through lowered pH and the creation of decay-resistant litter (Malmer et al., 2003). In addition, although thawed OM is more available to microbial decomposition, inundation creates an anaerobic low nutrient environment, which shifts microbial populations toward less efficient anaerobic metabolism and the production of CH_4 rather than CO_2 (Treat et al., 2014). When present, *Carex* spp. are known to increase release of these gases to the atmosphere from deeper in the soil profile through their aerenchymatous tissues (Waldo et al., 2019).

Permafrost thaw and the formation of collapse-scar bogs alters net ecosystem exchange, as evidenced by the amount of C stored within peat. Some studies have found large C losses from thawed permafrost peat (Jones et al., 2017; O'Donnell et al., 2012) and suggest that it may take centuries to millennia for these C stocks to recover to their pre-thaw stocks. However, other studies have shown little C loss from previously frozen peat (Estop-Aragonés, Cooper, et al., 2018; Heffernan et al., 2020), such that these losses could be relatively quickly offset by post-thaw peat accumulation. Regional differences in climate, geomorphological setting, and permafrost history could account for the observed variations in permafrost C dynamics among the studies measuring post-thaw C loss. In addition, different measurement techniques (i.e., chronosequence-based changes in C stocks vs. atmospheric flux measurements) may also account for disparate outcomes. In contrast to the stock method, flux measurements do not account for C losses due to winter losses, which can be significant (Natali et al., 2019; Waldrop et al., 2021) nor lateral flow, although measured C loss due to this flow appears to low (Hugelius et al., 2020; Tanentzap et al., 2021). To further understand the factors that determine the magnitude of C lost upon permafrost thaw, this study examines C losses for a thaw chronosequence at a site located in Interior Alaska. We calculate the amount of C loss with thaw for this site and examine these results in context of similar studies to understand the factors driving C loss rates.

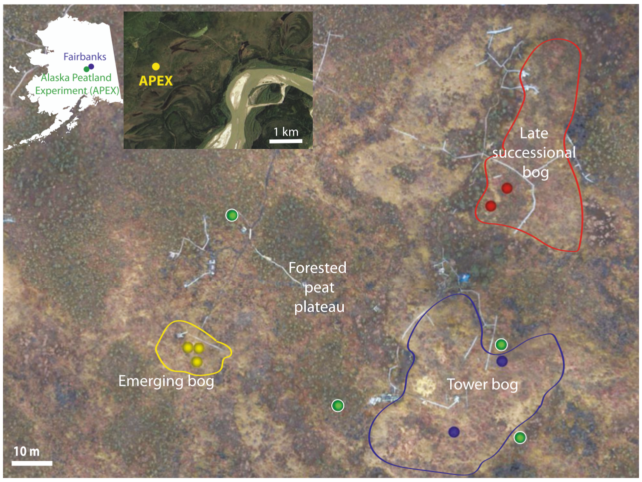

Figure 1. The Alaskan Peatland Experiment (APEX) site. This area is a mosaic of collapse-scar bogs within forested peat plateaus underlain by shallow permafrost. Colors correspond to the different bogs: the "Late Successional" bog is in red, the "Tower" bog is in blue, and the "Expanding" bog is in yellow. Circles indicate the locations of the soil cores; green/white circles are cores taken from the forested peat plateau. Core numbers can be found in Table S1 and Figure S2 in Supporting Information S1. APEX is located near Fairbanks, close to the Tanana River, in the Interior of Alaska. Images: site—J. Hollingsworth; satellite—Google Earth.

2. Methods

2.1. Site Information

This study took place in the Alaska Peatland Experiment (APEX; Figure 1), located within the lowlands of the Bonanza Creek Long-term Ecological Research (LTER) site, on the northwest side of the Tanana River, a glacially fed braided river. The average annual temperature for this part of Interior Alaska is −2.4°C (1981–2010), with the average January and July temperatures being −22.2°C and 16.9°C, respectively (http://www.ncdc.noaa.gov/cdo-web/datatools/normals; Fairbanks, AK). This region receives ~285 mm of precipitation per year, with about one-third occurring during the winter months (Hinzman et al., 2006). This region is also within the area of discontinuous permafrost; therefore, permafrost tends to be found on north facing slopes, in valley bottoms, and lowlands (Brown & Kreig, 1983).

The study area is dominated by forested peat plateaus, covered with *Picea mariana,* ericaceous shrubs, feather mosses, and occasional *Eriophorum* spp. in the wetter areas. These plateaus, which have shallow active layers (0.4–0.8 m) that are underlain by permafrost, are broken up by collapse-scar bogs of varying sizes (5–15,000 m^2). Collapse-scar bogs form when localized permafrost thaws; these wetlands remain surrounded by forested peat plateaus as well as have deeper permafrost below, isolating the thawed bog from groundwater. Vegetation of these bogs is characterized by diverse *Sphagnum* and *Carex* spp. plants. We examined three thaw features within the study area, assumed to have thawed at different times in the past based on their size and surface vegetation. One thaw feature (~1,300 m^2), with no visible dead trees, was assumed to be the oldest thaw feature of the three (Figure 1, red outline, referred to as the "Late Successional bog"). The second feature (~2,000 m^2) has drunken or dead trees on the surface, suggesting it thawed more recently. It also has an eddy covariance flux tower (Euskirchen et al., 2014; Figure 1, blue outline, referred to as the "Tower bog"). A much smaller feature (~50 m^2) was assumed to have initiated thaw within the past few decades and has been expanding during recent years (Figure 1, yellow outline, referred to as the "Expanding bog"). These sites were assumed to represent features with different ages of thaw. In addition, we obtained soil cores from both the interior as well as the edges of these features so that our data would represent a range of thaw ages, following previous chronosequence studies (Jones et al., 2017; O'Donnell et al., 2012).

2.2. Soil Core Collection and Analysis

Two to four cores were collected at each site (Table S1 in Supporting Information S1), with method depending upon ecosystem type and time of sampling. Frozen soil was cored with a Snow, Ice, and Permafrost Research Establishment (SIPRE) corer (~7.6 cm diameter; Rand & Mellor, 1985). Unfrozen material was usually collected using a "frozen finger." Here, a thin-walled, hollow aluminum tube (~6.5 cm diameter), sealed at one end, was inserted into the peat to the mineral soil. A slurry of dry ice and ethanol was poured into the corer, freezing the surrounding material to the outside of the corer. After removal the exterior of the core was scraped to remove large roots and any foreign material that became frozen to the core during removal. Both SIPRE cores and frozen finger cores were taken to at least the peat-mineral soil boundary. Because the frozen finger corer did not always recover the surface ~20 cm of peat very well, we sometimes sampled surface material by removing the surface peat in blocks of known dimensions (peat monolith). When more than one method was used to collect a core, sample data were later combined to represent an entire soil profile. In all cases, cores were subsampled into 2–5 cm depth increments.

Processing steps for each subsample depended on the type of sample. Most SIPRE subsamples, which were a circular disk-shape, were divided into four quadrants used for: (a) chemistry (C, nitrogen (N), and ^{210}Pb) and bulk density, (2) macrofossil and ^{14}C analysis, (3) DNA-based plant community assessment, and (4) an archive. Volume of the bulk density quadrant was determined by first calculating the area the quadrant (0.25 * area of a circle) averaging several measurements of the radius (using digital calipers) and multiplying this value by the average of several measurements of the disk thickness. Bulk density samples were then weighed, oven dried (65°C for organic samples, estimated to have >20% OM; 105°C for mineral soils), weighed again, and ground to pass through a 0.25 mm screen for further analyses (see following paragraph). For other SIPRE subsamples the disk was trimmed into the shape of a rectangle, the dimensions of which were measured using digital calipers, with the remainder of the core saved for other analyses and an archive. Frozen finger samples had at least three small rectangular cubes cut from the larger sample, the dimensions of which were measured using digital calipers. The remainder of the frozen finger subsample was split between macrofossil analyses and an archive. The rectangular prisms from both the SIPRE and the frozen finger methods were dried and ground in the same manner as described above. Regardless of sample collection method, all samples were described using visual and tactical factors such as level of decomposition, color, and root abundance. Based on these descriptions they were assigned a horizon designation: live moss (L), dead moss (D), fibric (mostly undecomposed plant material, F), mesic (more decomposed plant material, M), humic (very decomposed plant material, H), and mineral soil (Min) based on Manies et al. (2020).

The chemistry sample was analyzed for total C and N using a Carlo Erba NA1500 elemental analyzer (ThermoScientific, Waltham, MA). Samples were combusted in the presence of excess oxygen. The resulting sample gases were carried by a continuous flow of helium through an oxidation furnace, followed by a reduction furnace, to yield CO_2, N_2, and water vapor. Water was removed by a chemical trap and CO_2 and N_2 were chromatographically separated before the quantification of C and N (Pella, 1990a, 1990b). Because carbonates are generally absent in this area and pH values were generally less than 6.0, it was assumed that there was no inorganic carbon present in the mineral soil samples (Soil Survey Staff, 1951), and, thus, total C represents total organic C. More detailed information regarding sample processing for samples from the Tower bog can also be found in Manies et al. (2017). C storage for each subsample was calculated using C concentration (%), bulk density (g cm^{-3}), and thickness (cm) data. C stocks (kg m^{-2}) were calculated as cumulative C storage for all samples between the moss surface and the organic-mineral soil interface. Examinations of C stocks versus the number of years for which the core had that stratum (i.e., was a fen, had permafrost) were performed using the *nls* and *lm* commands in R (R Core Team, 2017).

To date surface soil layers, we measured both ^{14}C in plant macrofossils (see below) and ^{210}Pb in bulk soil. ^{210}Pb is largely deposited from atmospheric fallout, largely during precipitation events. Age dating using this radionuclide assumes that ^{210}Pb does not migrate downward within the soil profile over time, so that the activity found at depth reflects its decay since time of deposition. To examine if ^{210}Pb was migrating we collected additional surface soil samples for which we measured both ^{210}Pb and ^{7}Be. Because ^{7}Be is also deposited atmospherically but has a much shorter half-life (53 days vs. 22 years), we used ^{7}Be as a tracer to estimate the amount of downward transport, or "downwash," of ^{210}Pb. Although ^{137}Cs was measured (data available in Manies et al., 2021), it was not used to date soil layers due its mobility in acidic peat and potential biological uptake by vegetation (Turetsky et al., 2004). More details regarding the methods used for radionuclide data can be found in the Supporting Information.

2.3. Macrofossil Analysis

Plant macrofossil assemblages were used as evidence for transitions from one state to another, such as a forested peat plateau to a collapse-scar bog. Approximately 2 cm^3 of sample was washed through a 250 μm screen using deionized water and examined under a microscope to identify dominant peat types using semi-quantitative methods (Yu, 2006). Relative abundances of herbaceous, ligneous, and bryophytic peat were estimated and seeds, needles, leaves, and other distinct plant macrofossils were tallied. Based on characteristics of macrofossil assemblages (Treat et al., 2016), we classified the peat into several categories: (a) "herbaceous"-dominated peat, containing remains of Cyperaceae (sedges); (b) "ligneous" (woody) peat assemblages, which included evidence for taxa such as black spruce (*Picea mariana*), shrubs, and bryophyte taxa (e.g., feather mosses) associated with hummocks; and (c) "bryophytic" peat, which was dominated by *Sphagnum* and brown mosses. Where possible, *Sphagnum* mosses were identified to section level and brown mosses were identified to genus or species level. Brown mosses were further categorized based on their habitat. For example, mosses in the Amblystegiaceae family are associated with inundated environments, while feather mosses, *Tomentypnum nitens*, and *Aulacomnium palustre* were grouped into a "dry" (hummock or forest peat plateau) category. Unidentifiable detritus, or plant remains that were too decomposed to identify their provenance, was also included when present. Zones of permafrost aggradation (a transition from fen/marsh peat to plateau peat, see Section 3) were identified using a decrease in herbaceous peat with a corresponding increase in ligneous peat. Zones of permafrost thaw (collapse-scar bog peat) were identified using an increase in bryophytic peat with a corresponding decrease in ligneous peat. Transitions between peat types were identified using visual inspections of the macrofossil data and confirmed with CONISS based cluster analysis using the Tilia program, which clusters samples based on presence and abundance of taxa in each sample (v 2.6.1; Grimm, 1987). Core sections with "dry" mosses, even in small percentages, were assigned to the forested peat plateau strata. Note that macrofossil horizon designations are not synonymous with field-based horizon designations (e.g., fibric, mesic, and humic).

Macrofossil material was used to obtain radiocarbon (^{14}C) ages of peat initiation, permafrost aggradation, and permafrost degradation rates in each core. We picked terrestrial plant macrofossils (seeds, leaves, needles and charcoal) from the sieved macrofossil samples, targeting the depths of transition in macrofossil assemblage. The ^{14} C content of each sample was measured by accelerator mass spectrometry at either the Lawrence Livermore National Laboratory Center for Accelerator Mass Spectrometry (CAMS) or at Beta Analytic (Miami, FL; see Table S2 in Supporting Information S1 for details). Additional information regarding ^{14}C processing can be found in Manies et al. (2017). Radiocarbon ages were calibrated to ages in calendar years before present (cal yr BP; present = 1,950 CE) and age models were generated using Bacon v 2.3.9.1 (Blaauw & Christen, 2011).

2.4. C Loss Over Time

Cores from the same location (within 100 m of each other) have variable amounts of C in their permafrost strata for two reasons: (a) loss due to thaw, and (b) differing amounts of time for which a core had permafrost, which affects the total amount of forest peat plateau C that a core was able to accumulate. We accounted for the variable times for which cores had permafrost in two ways. The first method normalizes the C stocks of each of the thawed cores based on the amount of time each core was accumulating non-collapse scar bog peat (i.e., peat from the fen/marsh and forested peat plateau stratums, which accumulated before permafrost degradation) in relation to the longest amount of time a core was recorded as accumulating these peats (2,725 years). For example, the Expanding bog core-2 core accumulated both fen/marsh and forested plateau peat for 2,040 years, or 75% of 2,725 years. Therefore, we increased the C stocks of this core by 25%, thus accounting for any differences in stocks that may have occurred due to differences in time, with the assumption that any remaining differences in C stocks are due to thaw-based C losses. We are calling this process the "Normalized C" method. Confidence intervals were determined using the R package *plotFit* (Greenwell & Schubert Kabban, 2014).

The second method we used to account for C stock differences was also used by Jones et al. (2017). In this method two linear relationships between C stocks versus time (years with fen and permafrost peat) are calculated for (a) for the cores for which permafrost is still present and (b) for the cores for which permafrost has thawed. The difference between these two slopes indicates the degree to which C has been lost with thaw. We are calling this process the "slope comparison" method.

For these analyses we chose to include both the forested peat plateau and fen/marsh stratums as both experienced lower rates of decomposition when permafrost was present. In addition, by including all peat not derived from collapse scar bogs in our analyses our results are more similar to other studies, allowing us to compare findings (see Section 3).

2.5. Plant DNA Extraction, Amplification, and Analyses

We used DNA based techniques to assess the relative abundance of plant DNA (Alsos et al., 2016; Taberlet et al., 2006), and compared it to morphologically-based macrofossil count data for four cores. For each of the four cores for which both macrofossils and DNA analysis was performed, we extracted total genomic environmental DNA (eDNA) from 44 samples, between 7 and 10 subsamples for each core from both above and below the macrofossil-identified transition from forested peat plateau to bog, along with eight negative controls (sensu Leewis et al., 2020). Whole genome eDNA was extracted from ~0.5 g of permafrost using the DNeasy PowerSoil Kit (Qiagen, Redwood City, CA) and DNA quantity was assessed using a PicoGreen dsDNA Assay Kit (Thermo Fisher Scientific Technologies, Wilmington, DE). We then amplified and sequenced the short and variable P6 loop region of the chloroplast *trnL* intron (Taberlet et al., 2006). Sequence reads were processed using the OBItools software package (Boyer et al., 2016; http://metabarcoding.org/obitools) with a few modifications.

Taxonomic assignment of sequences was performed with a local taxonomic reference library containing arctic and boreal vascular and bryophyte taxa (Alsos et al., 2016), after checking that reference taxa were consistent with the NCBI taxonomy scheme (accessed February 2019). Further details of core cleaning, PCR primers, thermocycler settings, and bioinformatic processing are given in the Supplemental Information. All sequence data have been deposited in the NCBI Short Read Archive under Bioproject #PRJNA726580.

Because of the large variation of values found for individual taxa we combined these data into families for a CONISS-based cluster analysis using Tilia in the same manner as with the morphological macrofossil analysis (v 2.6.1; Grimm, 1987). We defined the transition between bog and forest peat plateau vegetation using this sequence data as the depth at which the CONISS analysis first divided the data into different hierarchies, or clusters within the dendrogram.

3. Results

3.1. ^{210}Pb and ^{7}Be Results

We found that ^{210}Pb age estimates for many of the soil horizons were younger than ^{14}C-based dates (Table S2 in Supporting Information S1). We also found movement of ^{7}Be as deep as 7 cm (Figure S1 in Supporting Information S1), suggesting that there was downwash of both ^{7}Be and ^{210}Pb into the soil profile. This result is supported by the fact that we also found unsupported ^{210}Pb activity as deep as 75–135 cm within the soil profile (Manies et al., 2021). Downwash biases the mean accumulation rate toward higher values which, in turn, results in younger estimated ages at a specific horizon. Attempts to account for the effect of downwash on ^{210}Pb age dating using two different models were unsuccessful (Manies et al., 2016). Therefore, we did not use ^{210}Pb data in our age models, but instead only use ^{14}C measurements of macrofossils for age modeling.

3.2. Site History

Age model results from the nine cores, all located within the 0.2 km^2 study area, reveal that the onset of peat formation began at the study site between −700 and 500 CE (Table 1). Sites closer to the Tanana River are younger by several 100 years (Figure S2 in Supporting Information S1), suggesting that, even within this site's small footprint, peat formation was influenced by the retreat of the river. Plant macrofossils indicate that peat is dominated by herbaceous material, typically from sedges (Cyperaceae) and ericaceous plants (Figures 2 and S7 in Supporting Information S1), indicating that this site was initially dominated by fen and marsh vegetation. Much of the peat within the fen-marsh stratum was classified as plant detritus, indicating this peat's C is highly processed. This marsh/fen stratum was present at the base of all cores.

Above the marsh/fen stratum, all cores transitioned to plant macrofossils dominated by ligneous peat (e.g., black spruce roots or needles, ericaceous shrub roots, and leaves; Figures 2 and S7 in Supporting Information S1). The transition between herbaceous and ligneous peat indicates when permafrost first aggraded at the site, ~1450–1770 CE. Cores from the collapse-scar bog also had a surficial stratum dominated by bryophytic peat (*Sphagnum*-dominated, with occasional appearance of brown mosses and Cyperaceae) consistent with permafrost thaw (Figures 2 and S7 in Supporting Information S1). Age models suggest that permafrost thaw began between 1874 and 1954 CE (Table 1). Because cores were taken in different locations within each feature (e.g., center and edge) we can use these data to understand how these features expanded. We expected the Tower bog to have formed more recently than the Late Successional bog, which does not appear to have been the case (Figure S3 in Supporting Information S1). To confirm this finding we

Table 1
Estimates of Year of Peat Formation, Permafrost Aggradation, and Permafrost Thaw

Site	Core	Peat initiation (CE)	Year of permafrost aggradation (CE)	Year of permafrost thaw (CE)
Expanding bog	BZBB 2	−110 (−226 to 34)	1447 (1285–1577)	1933 (1825–1971)
	BZBB 3	−203 (−607 to 118)	1469 (1139–1671)	1999 (1983–2011)
	BZBB 4	−468 (−668 to −376)	1710 (1676–1767)	1936 (1868–1976)
Tower bog	BZBT 1	42 (−50 to 196)	1601 (1475–1766)	1954 (1752–1981)
	BZBT 9	494 (144 to 952)	1769 (1689–1855)	1976 (1969–1986)
Late Successional bog	BZSE 3	−49 (−514 to 408)	1563 (1402–1756)	1994 (1981–2004)
	BZSE 4	−156 (−195 to −100)	1710 (1541–1746)	1874 (1705–1846)
Forested peat plateau	BZPP 11	84 (−478 to −464)	1623 (1473–1769)	—
	BZGC 11	−711 (−910 to −508)	1675 (1464–1808)	—

Note. Age estimates are based on Bacon age model results (Figure S8 in Supporting Information S1) using radiocarbon data (Table S2 in Supporting Information S1) for the depths at which transitions between stratums were noted using macrofossils (Figure S7 in Supporting Information S1).

examined images of the area from 1969 (Declassified CORONA Satellite Imagery, 2.75 m resolution) and 1994 (air photos, Scale 1:17,000), comparing the relative size of these two bogs between these images. This rough appraisal confirmed that these two features were mostly formed by 1969 with slight expansion up to 1994 and present day.

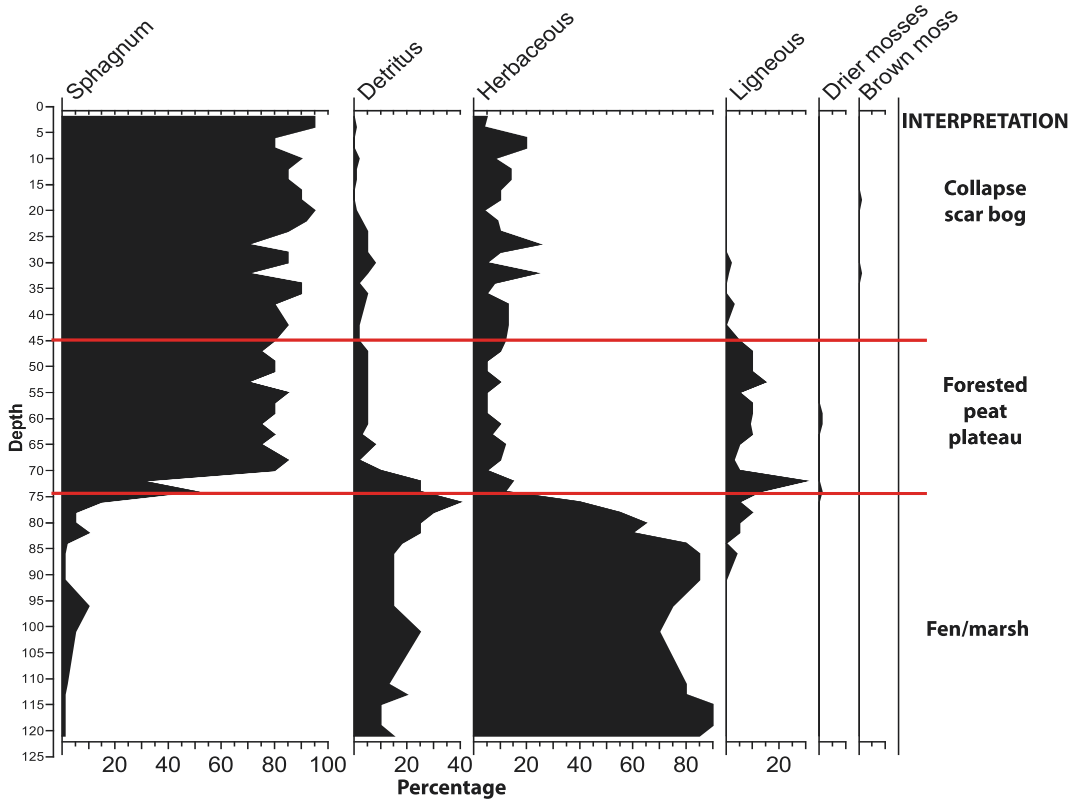

Figure 2. Simplified macrofossil diagram showing how changes in different amounts of material were used to determine the transitions between stratum ecosystems. Collapse scar bogs were dominated by bryophytic peat, while forested peat plateaus had high levels of ligneous peat. At the base of all cores was material dominated by herbaceous peat from the initial fen/marsh period. This diagram is for the core Expanding bog-4. Full macrofossil diagrams can be found in Figure S7 in Supporting Information S1.

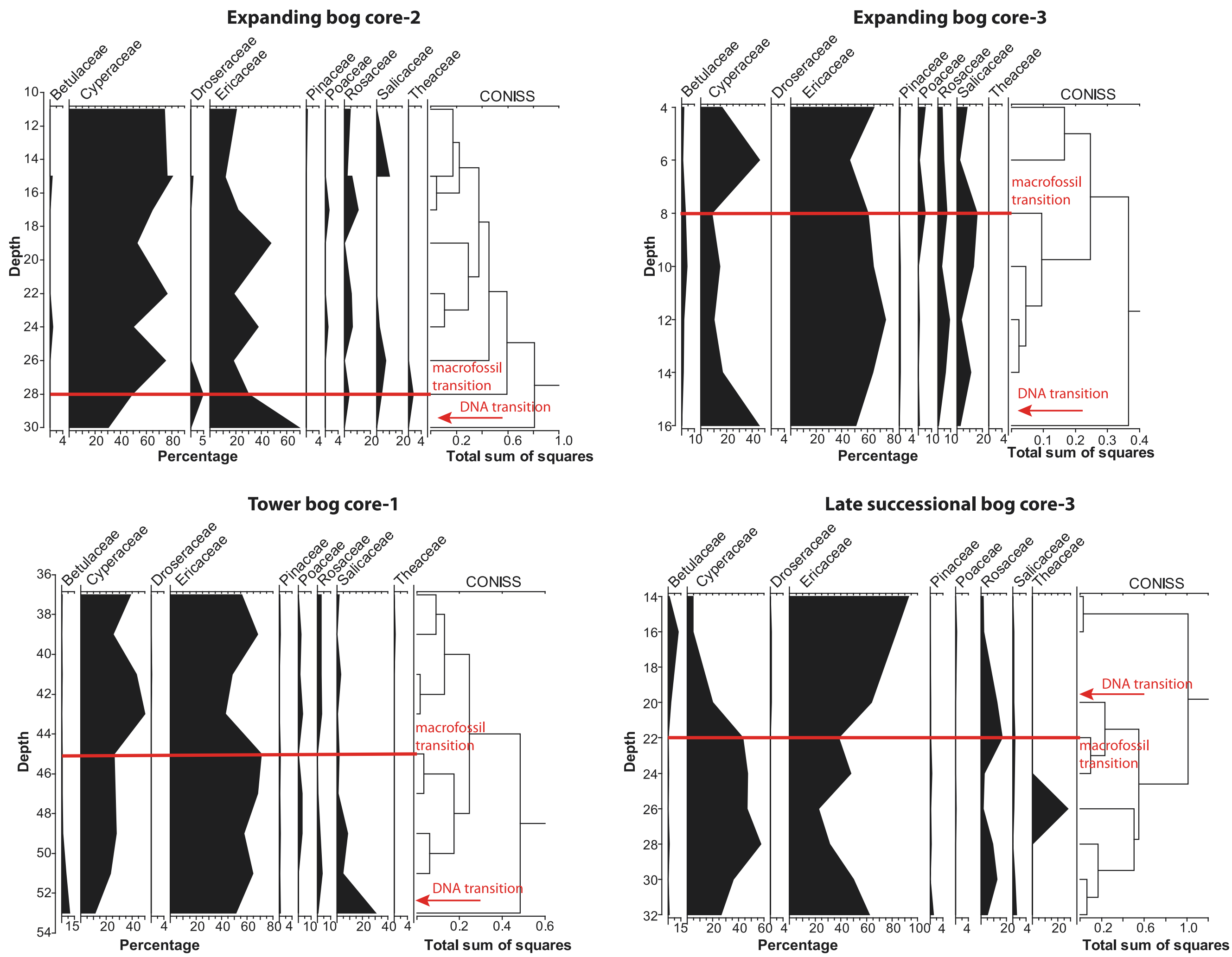

Figure 3. Vegetation transition analysis from peat cores using CONISS analysis of plant DNA at the family level. The red lines indicate the depths of macrofossil-based strata transitions, while the red arrows indicate where the CONISS analyses indicates the first break in the DNA data.

3.3. Macrofossil—DNA Comparison

Similar to macrofossils, the relative abundance of the chloroplast nucleic acid biomarker (*trnL*) showed changes in vegetation composition with depth for all cores. Some of the main vegetation classes found in the DNA data align with macrofossils found in relatively high abundance (for example, Betulaceae, Cyperaceae, and Ericaceae). However, even though mosses, especially *Sphagnum* spp., were often a large component of the macrofossil data, none of the moss species identified in the macrofossils were identified in the extracted and sequenced DNA. Missing vegetation in DNA analyses, mostly arboreal and *Sphagnum* species, has also been noted by others (Birks & Birks, 2016; Zimmermann et al., 2017). These missing taxa may be due to issues of primer bias, DNA degradation, plant protection of DNA, database representation, and/or DNA extraction efficiency (Parducci et al., 2015). We used the CONISS method (Grimm, 1987), a stratigraphically constrained cluster analysis, to determine where the DNA-based data transitioned from a forested peat plateau to a collapse scar bog and compared these values to the macrofossil-based depths. Of the four cores for which we have both *trnL* DNA and morphological-macrofossil data, two of the DNA dendrograms showed a first-level split into clusters at a similar depth as the macrofossils (Figure 3, Expanding bog-2 and Late Successional bog-3). In the other two cores the DNA-based depth of transition did not match the macrofossil-based depth (Expanding bog-3 and Tower bog-1). If we relied on the DNA-based first level split the differences in transition depths would have changed the estimated C stocks in the thawed bog stratum −3.2 to 0.5 kg m^{-2}, which is up to a 30% difference. Because the main identifier of collapse-scar bog

Table 2
C Storage (kg m^{-2}) for the Three Different Core Strata (Fen/Marsh, Forested Peat Plateau, and Collapse-Scar Bog Peat) Representing the Three Different Periods This Site Has Experienced (Post-Floodplain Vegetation, Permafrost Aggradation, and Post-Thaw)

		Carbon stocks (kg C m^{-2}) in peat			
Site	Core	Fen/marsh	Forested peat plateau	Collapse-scar bog	Total stocks
Expanding bog	BZBB 2	16.4	12.2	3.0	31.7
	BZBB 3	42.4	12.6	0.7	55.6
	BZBB 4	22.2	7.0	9.7	38.9
Tower bog	BZBT 1	29.0	4.6	7.4	41.0
	BZBT 9	26.4	11.4	4.9	42.7
Late Successional bog	BZSE 3	17.5	5.5	1.5	24.6
	BZSE 4	22.0	5.5	10.7	38.2
Forested peat plateau	BZPP 11	26.5	12.0	—	38.5
	BZGC 11	80.1	13.0	—	93.1

Note. The forested peat plateau does not have bog peat because these areas still contain permafrost.

peat is the presence of moss species like *Sphagnum angustifolium* and *Sphagnum riparium,* we chose to only use the macrofossil approach to determine stratigraphic boundaries.

3.4. C Stocks and Loss With Thaw

Total peat C stocks (to mineral soil) ranged from 24.6 to 93.1 kg m^{-2}, but this C was divided between two and three stratums, depending on location of the core. Stocks of C of the fen/marsh stratum ranged between 16 and 42 kg C m^{-2}, with one core having 80 kg C m^{-2} (Table 2). There was a moderate logarithmic relationship between the amount of C within the fen/marsh stratum and the number of years the core was a fen/marsh ($a = 2.27$, $b = -14.65$, goodness of fit = 0.49, Figure S4 in Supporting Information S1). C stocks for the forested peat plateau stratum ranged between 4.6 and 13.0 kg C m^{-2} (Table 2) and also had a moderate logarithmic relationship between C stocks and number of years with permafrost ($a = 0.7575$, $b = 4.96$, goodness of fit = 0.69, Figure S4 in Supporting Information S1).

When C loss due to thaw was examined using normalized stocks, we found a loss of C in the century following permafrost thaw of 34%, or 20 kg m^{-2}, with a range of 8%–60% (95% confidence intervals: Figure 4a). When using the slope method to compare C stocks of cores from the forested peat plateau, where the peat remains frozen, to the non-bog peat for cores where permafrost has thawed (Figure 4b), we find a 46% decrease in C (Figure 4b), which, if peat has accumulated for 2000 years means a C loss of 27 kg m^{-2}. However, because the line for still frozen peat is based on only two cores the error associated with its equation is large, such that there is high uncertainty with estimate. If we compare results of the linear method for APEX to those of Innoko, AK, which is of a similar age but formed permafrost syngenetically with peat accumulation (Jones et al., 2017, Figure 4b), we observe both lower C accumulation in APEX than Innoko as well as smaller losses. Thus, C losses (kg m^{-2}) at APEX are over 50% less than found at Innoko. The slope method has two assumptions: (a) peat C at initiation is zero and (b) peat accumulates linearly with time. A linear relationship may not be a true representation of peat accumulation but the short time span between permafrost initiation and thaw at APEX precludes us from determining the nature of this relationship (i.e., logarithmic, exponential, etc.)

Stocks of post-thaw collapse-scar bog peat ranged between 0.7 and 10.7 kg C m^{-2}. While we found a moderate logarithmic relationship between the amount of C and the number of years for which the core was a collapse-scar bog (goodness of fit = 0.60), the initial accumulation rates for this model were unreasonable (>3 kg m^{-2} yr^{-1}). Therefore, a polynomial relationship appears to better represent our data (intercept = −0.1551, $x = 0.1996$, $x^2 = -0.0003$, adjusted $r^2 = 0.64$; Figure S4 in Supporting Information S1).

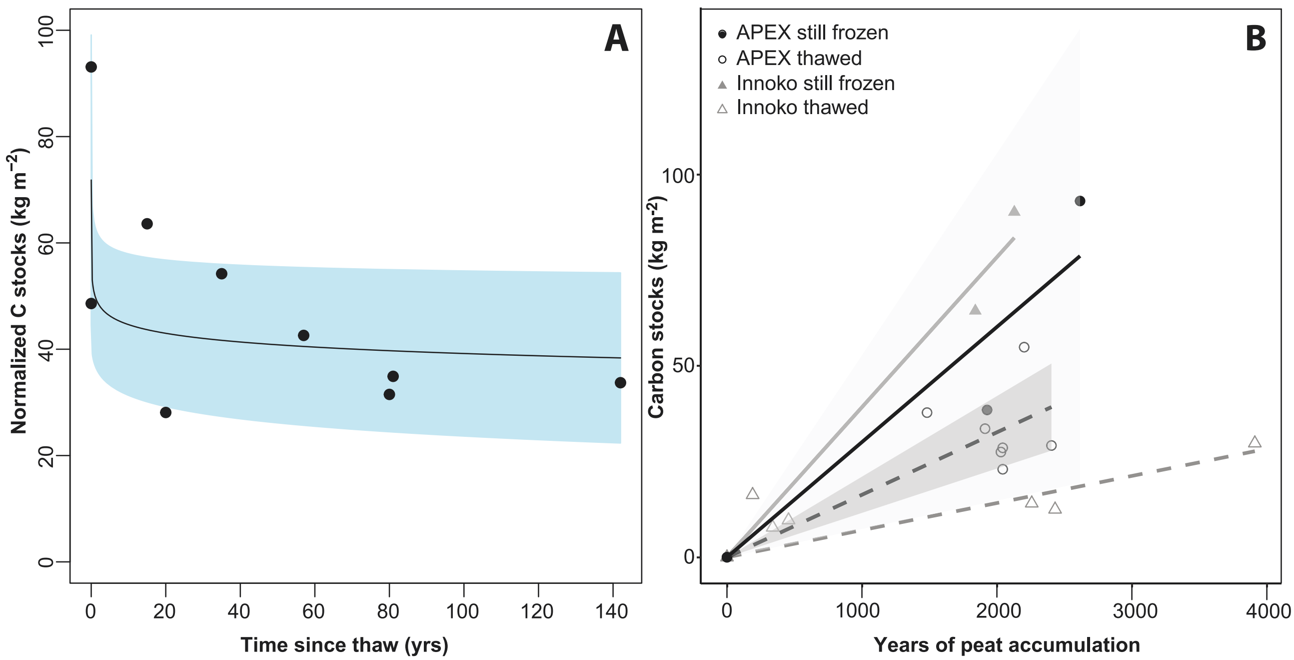

Figure 4. Estimating carbon losses from APEX permafrost using two methods. (a) The Normalized C method, where C stocks were normalized to the oldest core and then plotted against the number of years each core has been thawed (see methods). This method shows a 34% loss of C with time. (b) The linear method comparing stocks between still frozen peat (solid lines) and thawed peat (dashed lines) for both the APEX site (black, this study) and Innoko, AK (gray, Jones et al., 2017). With C loss, the slope of the line representing thawed cores (dashed line) will have a lower slope than the slope of the line where the cores still contain permafrost (solid line). Using this method APEX C losses are estimated at 46% of the existing stocks, with absolute C losses (kg C) lower than found for Innoko. However, the error associated with frozen core data is large (shading), creating higher uncertainty in the values calculated using this method.

We calculated net C gains/losses by summing C gains with post-thaw moss peat growth (Figure S4 in Supporting Information S1) with losses with thaw, using logarithmic relationships for permafrost C loss with thaw (Figure 4a). Results suggest that the site experienced net C losses in the first 10 years following thaw, but post-thaw peat accumulation resulted in net C gains thereafter (Figure 5). Carbon stocks reached their pre-thaw levels within 150 years, regardless of the number of years we model for pre-thaw peat accumulation (Figure 5).

3.5. C:N Ratio Comparison Between APEX and Innoko

C:N ratios can be indicative of how decomposed plant residues are, as C:N ratios typically decline during the decomposition processes, especially when examined within a vegetation or ecosystem type (Treat et al., 2016). Syngenetic permafrost would, therefore, be expected to have higher C:N ratios than quasi-syngenetic or epigenetic permafrost because in syngenetic permafrost the plant tissue was entrained in permafrost before much processing through decomposition could occur. In contrast, quasi-syngenetic permafrost and epigenetic permafrost forms after peat formation, incorporating peat that has already been exposed to microbial processing. To determine how well nutrient concentrations work in this capacity we compared the C:N ratios, as well as concentrations of C and N, from APEX, which contains quasi-syngenetic permafrost, to Alaskan sites with syngenetic permafrost peat (Innoko and Koyukuk NWR; Jones et al., 2017). An ANOVA (*aov* command; R Core Team, 2017) was used to compare these values between sites and among organic soil horizons. The soil horizons (fibric, mesic, and humic) (Manies et al., 2020) are based on visual quantifications of the degree of decomposition within the soil sample, not a detailed macrofossil analysis. We found that permafrost type ($p < 0.001$, $F = 62.16$), but not horizon code nor a permafrost by horizon code interaction, had a significant effect on C:N ratios. Subsequent statistical comparison of C found similar results, with permafrost type being the only significant factor ($p < 0.001$, $F = 88.3$), with epigenetic permafrost having lower C concentrations than syngenetic permafrost (31.3 vs. 41.2% C, respectively, Figure S6 in Supporting Information S1). Permafrost type was also a significant factor for N concentrations ($p < 0.001$,

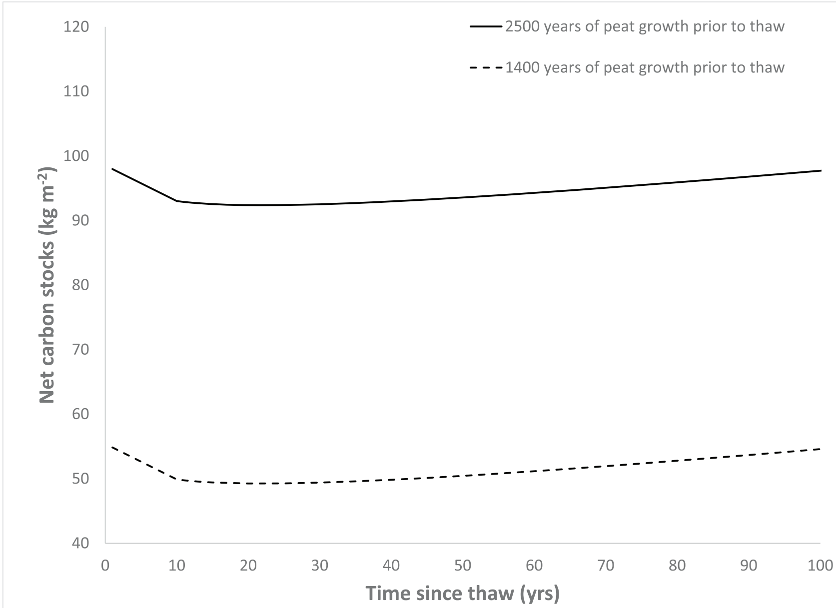

Figure 5. Net C stocks, modeled as inputs from bog C and losses due to permafrost thaw for two time periods, which represent the upper and lower estimates of times at which peat initiated.

$F = 19.0$), with epigenetic permafrost having higher N than syngenetic permafrost (1.6 vs. 1.3% N, respectively, Figure S6 in Supporting Information S1). In addition, there was a permafrost by horizon interaction ($p < 0.03$, $F = 4.7$), with mesic epigenetic permafrost having higher N concentration that humic epigenetic permafrost (1.8 vs. 1.3% N, respectively, Figure S6 in Supporting Information S1).

4. Discussion

4.1. Site History

The APEX research site experienced permafrost thaw within the last century, resulting in the formation of multiple thermokarst bogs of different ages. The paleoecological history of the site has been influenced by local flooding due to its proximity to the Tanana River. Large floods occurred along the Tanana River from −1,050 to −50 CE (Mason & Begét, 1991), which coincides with the timing of peat initiation at this site (−710 to −500 CE; Figure S2 in Supporting Information S1), suggesting that a combination of a decrease in river flooding and a movement of the river away from the study site allowed for peat initiation to begin. Variability in peat initiation ages is likely related to differences in local microtopography and hydrology as the Tanana River moved away from the site, with locations to the north and the west of the site (e.g., peat plateau core GC11) initiating before areas to the south or east (Figure S2 in Supporting Information S1). Macrofossils reveal that these sites existed as permafrost-free fens until permafrost aggraded between 1,450 and 1,775 CE (Table 1), which corresponds to one of the maxima of the Little Ice Age (LIA; Miller et al., 2012). This timing is also consistent with broader scale Holocene climatic changes that resulted in a general increase in the aggradation of permafrost in northern peatlands ~1,000 years ago, culminating during the LIA (Treat & Jones, 2018).

We were surprised to find that the age of permafrost thaw did not correlate to thaw feature size. While thaw in the Late Successional bog appears to have begun thawing decades before the two other bogs, the Expanding and Tower bogs appear to have begun thawing around the same time (Table 1). What differs between these two bogs is how fast the feature expanded; the Expanding bog remained small for decades and only recently has begun expanding, while the Tower bog appears to have been expanding since thaw began in the 1950s (Figure S3 in Supporting Information S1).

Several reasons could explain the difference in how fast these bogs expanded. One factor could be differences in ice content, as permafrost with high ice content is at greater risk of thaw resulting in thermokarst

(Olefeldt et al., 2016; Shur & Jorgenson, 2007). High ice content soil is often associated with fine-grained surficial deposits (Jorgenson & Osterkamp, 2005). The proximity of the APEX site to the Tanana River suggests that, as the river meandered away, areas that were located in low-energy environments could have received higher amounts fine-grained sediment and, thus, could have higher mineral soil ice content. These localized areas of greater ground ice content could cause differential rates of bog expansion upon thaw. To investigate this hypothesis, we examined the volumetric water content (VWC), which would be higher in soils with more ice, of mineral soils below the active layer for cores taken around the site. The VWC content of cores taken near to the Expanding bog was lower ($p = 0.006$, Figure S5 in Supporting Information S1) than cores taken near the Tower bog, which experienced much quicker expansion (VWC 57.3 ± 11.4% vs. 64.6 ± 15.6%, respectively, mean ± SD).

Another factor that could have impacted the rates at which the Expanding and Tower bogs expanded is soil temperature. Data from Waldrop et al. (2021) show that in September 2015 the deep peat at the Tower bog was warmer than the deep peat at the Expanding bog. Neumann et al. (2019) demonstrated that the temperature of rain and any resulting subsurface flow can impact deep soil temperatures, especially at bog edges. Therefore, if the Tower bog received more water inputs from the surrounding forested peat plateau than the Expanding bog these additional inputs could have resulted in warmer peat temperatures, which in turn could have expanded the Tower bog faster than the Expanding bog. Macrofossils support this hypothesis, as cores from the Tower bog show the presence of brown mosses, which suggests more mineral/nutrient input, such as through groundwater or overland flow. These mosses were not found in the cores from the Expanding bog.

External factors, such as wildfire and solar based thermal inputs could also explain the expansion differences between the Expanding and Tower bogs. Both bogs have some cores with horizons dated from the past two centuries (when thaw began in this area) that contain charcoal. Therefore, although it is possible that fire played a role in advancing permafrost thaw at these bogs, it is not likely. Although the features are surrounded by similar vegetation, local differences in shading at the areas of initial thaw between the Expanding and Tower bog could have impacted thaw rates. However, ice content and/or water inputs likely played a larger role in these different rates of growth.

4.2. Plant DNA-Based Stratigraphy

Many studies have demonstrated that DNA-based analyses, such as sequencing of the *trnL* chloroplast intron, can be used to understand long-term paleoecological changes in vegetation similar to macrofossils (i.e., thousands of years; Parducci et al., 2015, 2017; Zimmermann et al., 2017). Our DNA-based reconstruction identified fewer taxa than identified by the macrofossil analysis, as is consistent with the literature (see Figure 2 of Parducci et al., 2015). Changes in moss species is a key indicator of thaw, both in the field and in macrofossil analyses, but was mostly absent from our DNA analyses. We identified three potential reasons for this under-representation of bryophytes in the sequence-based data set. First, the primers used targeted the P6-loop of the chloroplast *trnL* (UAA) intron, which is a universal, short, plant-specific biomarker. Although these same primers have been shown to successfully amplify and identify *Sphagnum* spp. from Arctic sediment cores, *Sphagnum* are not the main target of these primers and, therefore, amplification may be biased against inclusion in a *trnL* sequence-based dataset (Alsos et al., 2016; Zimmermann et al., 2017). Second, the identification of sequences species relies on the completeness of the reference database. We used European arctic/vascular and bryophyte databases, because as of yet no Northern American arctic/boreal plant database with the chloroplast *trnL* (UAA) intron exists. The only Sphagnum species within this database that is prominent at our site is *Sphagnum riparium*. The lack of representation of other Sphagnum species that are commonly found in Alaska (Vitt et al., 1988) within this database could have caused bias against the identification of local *Sphagnum* spp. Finally, when *Sphagnum* biomass is buried cell lysis and the presence of secondary metabolites may increase the rate of DNA degradation (Xie & Lou, 2009). We believe with further improvement this method could be more useful for paleoecological studies of Alaskan flora and, potentially, though inclusion of *Sphagnum* specific primers, useful for identification of vegetation transitions across broad time scales.

We were interested in knowing if these DNA based methods could be used to mark finer-scale (decadal) transitions between vegetation, such as when permafrost thawed and forested peat plateaus transitioned

10.1029/2021JG006396

into inundated wetlands, as this determination using macrofossil data is a time- and training-intensive process. Identification of stratigraphic transitions between bogs and forest peat plateaus using the *trnL* amplicon only matched (within 2 cm) morphological identification-based transitions in two of the four cores we examined. We should note that due to time and sample constraints, we only conducted DNA-based analyses on ∼20-cm sections of each core, focused on the area where macrofossil data indicated a vegetation community shift occurred. Even considering this constraint, because the *trnL* vegetation reconstructions using the methods detailed herein do not consistently match macrofossil results we feel they are better used as a complementary tool, one that could be used as a "first pass" in paleoecological studies, in conjunction with morphological macrofossil analyses, or when examining vegetation shifts across an entire core, representing tens of thousands of years of ecosystem change.

4.3. Estimating C Losses in Millennial Aged Permafrost

The magnitude of post-thaw C loss of lowland peatlands remains a matter of debate. While some studies have found large permafrost C losses due to permafrost thaw (Jones et al., 2017; O'Donnell et al., 2012), others show little to no loss, such that any losses can be relatively quickly recouped with post-thaw peat accumulation (Cooper et al., 2017; Estop-Aragonés, Cooper, et al., 2018; Estop-Aragonés, Czimczik, et al., 2018; Heffernan et al., 2020). We found evidence that between 34% and 46% of the C available at APEX was lost due to thaw (Figure 4). However, the errors in our dataset are relatively high, suggesting additional replicate cores and/or a chronosequence spanning a greater period of time would help constrain these values. We attribute the high scatter in the APEX dataset to natural landscape variability, the clustering of thaw ages within a few decades of each other, and radiocarbon calibration uncertainty associated with the timing of thaw coinciding with nuclear weapons testing. Additional sources of uncertainty include the small number of cores representing still frozen peat, the reliance on age models to date some transitions (due to lack of ^{14}C dates at the exact depth of transition), and the potential of mixing of macrofossil assemblages, which can happen due to edge slumping. Nonetheless, our data suggests that 20–27 kg C m^{-2} was lost due to thaw at APEX (normalized vs. linear method, respectively). These values are greater than the 9 kg C m^{-2} of losses found by Heffernan et al. (2020), but less than the 35–45 kg C m^{-2} of losses found by Jones et al. (2017). When comparing the APEX data with the data from Innoko, Alaska (Jones et al., 2017), which used similar methods for estimating C loss, we show that the Innoko forest peat plateaus both gained more C prior to thaw and lost more carbon following thaw compared to APEX (Figure 4b). We compared these two sites because peat initiated around the same time (Table 3; Figure 4b). We believe the main difference between these two sites is that Innoko contains syngenetic permafrost, where peat and permafrost accumulation happened simultaneously. In contrast, the permafrost at APEX was classified as quasi-syngenetic permafrost, a form of epigenetic permafrost. Quasi-syngenetic permafrost forms when the permafrost grows upward, like syngenetic permafrost, but incorporates already existing peat/sediments (Kanevskiy, 2003). Therefore, the permafrost at APEX aggraded following peat initiation and has only existed for several 100 years.

Differences in permafrost aggradation processes impacts how decomposed peat is, and, therefore, its chemical composition prior to its incorporation into permafrost (Treat et al., 2014). Because syngenetic permafrost is formed when permafrost aggradation and peat accumulation occur in tandem, syngenetic peat is less decomposed and, therefore, likely more susceptible to decomposition upon thaw. In contrast, epigenetic and quasi-epigenetic permafrost are formed with previously deposited sediments/peats, which have already been subject to microbial turnover and, therefore, likely decay more slowly upon thaw. High pre-permafrost C processing at APEX is evidenced by an abundance of detrital peat in the fen/marsh stratum (Figures 2 and S6 in Supporting Information S1), suggesting that the most labile fraction was processed prior to permafrost aggradation, rendering it less prone to further decomposition upon thaw. This result lies in contrast to the syngenetic permafrost peat plateaus at Innoko and Koyukuk NWR (Alaska), whose peat plateaus contained well-preserved peat in the permafrost (Jones et al., 2017; O'Donnell et al., 2012), subjecting it to rapid decomposition upon thaw.

Age factors, such as number of years a site has accumulated peat and had permafrost aggrading, also impact the amount of peat that has accumulated and, thus, the amount of C that can be lost due to thaw. Therefore, we compared these age factors, along with permafrost type, for studies that had examined C loss with permafrost thaw (Table 3). There was no consistent pattern between amount of C lost and age since peat

Table 3
Comparison of Common Factors for Studies That Have Seen Minimal Versus Large C Losses With Permafrost Thaw

Relative amount of C loss	Permafrost type	Peat initiation	No. of years permafrost present	No. of years permafrost thawed (approx.)	General location	Method
Smaller	Epigenetic (processed peat)	−450 to 550 CE (2,400–1,400 cal yr BP)	200–400	20–100	Fairbanks Alaska[a]	Chronosequence
Smaller	Epigenetic (processed peat)	−6,550 CE (8,500 cal yr BP)	1,800	30–200	AB, Canada[b,c]	Chronosequence and ^{14}C of gas
Smaller	Syngenetic and epigenetic (unprocessed and processed peat)	−5,550 to −4,650 CE (6,600–7,500 cal yr BP)	Unknown	20–130	NWT, Canada[d]	^{14}C-CO_2 of soil respiration
Larger	Syngenetic (unprocessed peat)	−6,050 to −8,050 CE (8,000–1,000 cal yr BP)	8,000–10,000	30–1,215	Koyukuk, Alaska[e,f]	Chronosequence
Larger	Syngenetic (unprocessed peat)	−1,050 to −50 CE (2,000–3,000 cal yr BP)	2,000–3,000	20–400	Innoko, Alaska[f]	Chronosequence

[a]This study. [b]Heffernan et al. (2020). [c]Estop-Aragonés, Czimczik, et al. (2018). [d]Estop-Aragones, Cooper, et al. (2018) and Wolfe and Morse (2017). [e]O'Donnell et al. (2012). [f]Jones et al. (2017).

formation. There was also no consistent pattern in number of years for which a site had permafrost and magnitude of C loss. However, we observed higher losses from sites with syngenetic permafrost and smaller losses from sites with epigenetic or quasi-syngenetic permafrost, suggesting that type of permafrost is an important factor in determining the relative amount of C loss due to thaw. Unfortunately, the one study site that contained both syngenetic and epigenetic permafrost (Estop-Aragonés, Cooper, et al., 2018) used a different methodology to look at C loss (^{14}C of soil respiration), precluding an examination into how the presence of both types of permafrost might influence C loss. At APEX, as in other studies with epigenetic peat (e.g., Heffernan et al., 2020), the relatively small C losses were recuperated within decades to centuries (vs. millennia) post-thaw.

The role that permafrost aggradation process plays suggests that better understanding of the spatial distribution of syngenetic and epigenetic permafrost could help constrain the landscape-scale magnitude of C loss from permafrost thaw in boreal peat plateaus. While the spatial extent of syngenetic versus epigenetic permafrost is not well documented, an analysis of permafrost aggradation timing relative to peatland age for circumpolar peat cores found that the majority of permafrost peatlands aggraded permafrost epigenetically within the late Holocene and as recently as the Little Ice Age (Treat & Jones, 2018), suggesting that C losses from thawing permafrost peatlands may be recovered relatively quickly overall. We must also recognize that soils can reflect complex sequences of different types of permafrost formation, with multiple types of permafrost found within the same location (Kanevskiy et al., 2014; Wolfe et al., 2014).

Due to the lack of permafrost type maps and the possibility of both syngenetic and epigenetic permafrost within a single core, other indicators need to be used to determine if thawing peat is susceptible to small or large C losses. Our results suggesting that C:N ratios would be a good first-order indicator of permafrost type align with the results others (Sannel & Kuhry, 2009; Schädel et al., 2014; Treat et al., 2016) In addition, C:N data are more accessible compared to macrofossil analyses, which require specialized training. The differences in C:N ratios between permafrost types is driven more by differences in C concentration (epigenetic = 31.3% vs. syngenetic = 41.2%; Figure S6 in Supporting Information S1) than N concentration (epigenetic = 1.6% vs. syngenetic = 1.3%; Figure S6 in Supporting Information S1). Epigenetic permafrost also has greater variability in C concentrations than syngenetic permafrost. Lower C concentrations for epigenetic permafrost are representative of the fact that its C has experienced more decomposition (Schädel et al., 2014) than syngenetic permafrost. Higher N concentrations in epigenetic peat may also be because this peat has experienced more decomposition prior to permafrost aggradation. Decomposition of peat reduces C concentrations and, thus, the overall concentration (%) of N in the peat may increase, even if the content (kg m^{-2}) of N does not. This idea is supported by the fact that there are higher N concentrations in mesic (less decomposed) horizons versus humic (more decomposed) horizons even within our epigenetic permafrost (1.81 vs. 1.50%, respectively, Figure S6 in Supporting Information S1). In addition, differences in vegetation composition (Treat et al., 2016) or fire history (Harden et al., 2002) can also affect N concentrations. The influence of these factors on these data is more difficult to determine.

5. Conclusions

We found that for the APEX site, located near the Tanana River of Interior Alaska, the timing of peat initiation was impacted by proximity to old river channels. Initially these sites were dominated by sedges and woody vegetation, consistent with rich fens that accumulated peat in the absence of permafrost. Permafrost aggraded at this site at the end of the Little Ice Age, consistent with observations of other permafrost peatlands in the discontinuous permafrost zone in Alaska. In the last century, permafrost began to degrade in places, transitioning some of the forested peat plateaus in this area into collapse-scar bogs. We found variable rates of bog expansion for the three different features studied herein and hypothesize that these differences are related to within-site differences such as ground ice content and the amount of overland flow received.

Using two different methods, we found smaller C losses post thaw (20–27 kg C m^{-2}) compared to other Alaskan locations. Based on a comparison of our results to other studies in the literature that also examined changes in permafrost C upon thaw, we conclude that in addition to age since peat initiation and length of time as permafrost, the permafrost aggradation process influences C loss with thaw. Areas where permafrost aggrades after peat formation (i.e., epigenetic) will experience less C loss with thaw, while sites that have syngenetic permafrost could experience large losses of C with thaw. Therefore, future research into changes in C loss with thaw should include determining the relative coverage of these permafrost types within the boreal region. Where this information is not known C:N ratios can be used to indicate the degree of processing of the peat, informing estimates of the degree of C loss with thaw.

Data Availability Statement

Data used in this study are available from Manies et al. (2021; https://doi.org/10.5066/P9AQOOTI).

Acknowledgments

We would like to acknowledge Yen Le for her help with the molecular analyses and Jack McFarland for advice and help efficiently sampling and subsampling these cores. Thanks to Mikhail Kanevskiy for his assistance in determining the type of permafrost found at APEX and to two anonymous reviewers, for their improvements to this manuscript. We also would like to acknowledge the assistance of the Fairbanks USGS office and the Bonanza Creek LTER, without which this work would not be possible. This work was funded by the USGS Climate and Land Use Change Program. Any use of trade, firm, or product names is for descriptive purposes only and does not imply endorsement by the U.S. Government.

References

Alsos, I. G., Sjögren, P., Edwards, M. E., Landvik, J. Y., Gielly, L., Forwick, M., et al. (2016). Sedimentary ancient DNA from Lake Skartjørna, Svalbard: Assessing the resilience of arctic flora to Holocene climate change. *The Holocene*, *26*(4), 627–642. https://doi.org/10.1177/0959683615612563

Birks, H. J. B., & Birks, H. H. (2016). How have studies of ancient DNA from sediments contributed to the reconstruction of Quaternary floras? *New Phytologist*, *209*(2), 499–506. https://doi.org/10.1111/nph.13657

Blaauw, M., & Christen, J. A. (2011). Flexible paleoclimate age-depth models using an autoregressive gamma process. *Bayesian Analysis*, *6*(3), 457–474. https://doi.org/10.1214/ba/1339616472

Boyer, F., Mercier, C., Bonin, A., Le Bras, Y., Taberlet, P., & Coissac, E. (2016). obitools: A unix-inspired software package for DNA metabarcoding. *Molecular Ecology Resources*, *16*(1), 176–182. https://doi.org/10.1111/1755-0998.12428

Brown, J., Ferrians, O. J., Jr., Heginbottom, J. A., & Melnikov, E. S. (1997). *Circum-Arctic map of permafrost and ground-ice conditions Circum-Pacific Map 45*. Retrieved from https://pubs.er.usgs.gov/publication/cp45

Brown, J., & Kreig, R. A. (1983). *Guidebook to permafrost and related features along the Elliott and Dalton Highways, Fox to Prudhoe Bay, Alaska*. Paper presented at the Fourth International Conference on Permafrost, University of Alaska.

Cooper, M. D. A., Estop-Aragonés, C., Fisher, J. P., Thierry, A., Garnett, M. H., Charman, D. J., et al. (2017). Limited contribution of permafrost carbon to methane release from thawing peatlands. *Nature Climate Change*, *7*(7), 507–511. https://doi.org/10.1038/nclimate3328

Estop-Aragonés, C., Cooper, M. D. A., Fisher, J. P., Thierry, A., Garnett, M. H., Charman, D. J., et al. (2018). Limited release of previously-frozen C and increased new peat formation after thaw in permafrost peatlands. *Soil Biology and Biochemistry*, *118*, 115–129. https://doi.org/10.1016/j.soilbio.2017.12.010

Estop-Aragonés, C., Czimczik, C. I., Heffernan, L., Gibson, C., Walker, J. C., Xu, X., & Olefeldt, D. (2018). Respiration of aged soil carbon during fall in permafrost peatlands enhanced by active layer deepening following wildfire but limited following thermokarst. *Environmental Research Letters*, *13*(8), 085002. https://doi.org/10.1088/1748-9326/aad5f0

Euskirchen, E. S., Edgar, C. W., Turetsky, M. R., Waldrop, M. P., & Harden, J. W. (2014). Differential response of carbon fluxes to climate in three peatland ecosystems that vary in the presence and stability of permafrost. *Journal of Geophysical Research: Biogeosciences*, *119*(8), 1576–1595. https://doi.org/10.1002/2014jg002683

Euskirchen, E. S., McGuire, A. D., Chapin, F. S., Yi, S., & Thompson, C. C. (2009). Changes in vegetation in northern Alaska under scenarios of climate change, 2003−2100: Implications for climate feedbacks. *Ecological Applications*, *19*(4), 1022–1043. https://doi.org/10.1890/08-0806.1

Finger, R. A., Turetsky, M. R., Kielland, K., Ruess, R. W., Mack, M. C., & Euskirchen, E. S. (2016). Effects of permafrost thaw on nitrogen availability and plant–soil interactions in a boreal Alaskan lowland. *Journal of Ecology*, *104*(6), 1542–1554. https://doi.org/10.1111/1365-2745.12639

Gibson, C., Estop-Aragonés, C., Flannigan, M. D., Thompson, D., & Olefeldt, D. (2019). Increased deep soil respiration detected despite reduced overall respiration in permafrost peat plateaus following wildfire. *Environmental Research Letters*, *14*. https://doi.org/10.1088/1748-9326/ab4f8d

Greenwell, B. M., & Schubert Kabban, C. M. (2014). investr: An R packages for inverse estimation. *The R Journal*, *6*, 90–100. https://doi.org/10.32614/rj-2014-009

Grimm, E. C. (1987). CONISS: A FORTRAN 77 program for stratigraphically constrained cluster analysis by the method of incremental sum of squares. *Computers & Geosciences*, *13*(1), 13–35. https://doi.org/10.1016/0098-3004(87)90022-7

Harden, J. W., Koven, C. D., Ping, C. L., McGuire, A. D., Camill, P., Jorgenson, M. T., et al. (2012). Field information links permafrost carbon to physical vulnerabilities of thawing. *Geophysical Research Letters*, *39*(15), L15704. https://doi.org/10.1029/2012gl051958

Harden, J. W., Mack, M. C., Veldhuis, H., & Gower, S. T. (2002). Fire dynamics and implications for nitrogen cycling in boreal forests. *Journal of Geophysical Research*, *107*(D3), WFX4-1–WFX4-8. https://doi.org/10.1029/2001jd000494

Heffernan, L., Estop-Aragonés, C., Knorr, K.-H., Talbot, J., & Olefeldt, D. (2020). Long-term impacts of permafrost thaw on carbon storage in peatlands: Deep losses offset by surficial accumulation. *Journal of Geophysical Research: Biogeosciences*, *125*(3), e2019JG005501. https://doi.org/10.1029/2019JG005501

Hinzman, L. D., Viereck, L. A., Adams, P. C., Romanovksy, v., & Yoshikawa, K. (2006). Climate and permafrost dynamics of the Alaskan boreal forest. In F. S. Chapin, III, M. W. Oswood, K. Van Cleve, L. A. Viereck, & D. Verbyla (Eds.), *Alaska's changing boreal forest* (pp. 39–61). Oxford University Press. https://doi.org/10.1093/oso/9780195154313.003.0008

Hugelius, G., Loisel, J., Chadburn, S., Jackson, R. B., Jones, M., MacDonald, G., et al. (2020). Large stocks of peatland carbon and nitrogen are vulnerable to permafrost thaw. *Proceedings of the National Academy of Sciences*, *117*(34), 20438–20446.

Jackson, R. B., Lajtha, K., Crow, S. E., Hugelius, G., Kramer, M. G., & Piñeiro, G. (2017). The ecology of soil carbon: Pools, vulnerabilities, and biotic and abiotic controls. *Annual Review of Ecology, Evolution, and Systematics*, *48*(1), 419–445. https://doi.org/10.1146/annurev-ecolsys-112414-054234

Jones, M., Harden, J., O'Donnell, J., Manies, K., Jorgenson, T., Treat, C., & Ewing, S. (2017). Rapid carbon loss and slow recovery following permafrost thaw in boreal peatlands. *Global Change Biology*, *23*(3), 1109–1127. https://doi.org/10.1111/gcb.13403

Jorgenson, M. T., & Osterkamp, T. E. (2005). Response of boreal ecosystems to varying modes of permafrost degradation. *Canadian Journal of Forest Research*, *35*(9), 2100–2111. https://doi.org/10.1139/x05-153

Jungqvist, G., Oni, S. K., Teutschbein, C., & Futter, M. N. (2014). Effect of climate change on soil temperature in Swedish boreal forests. *PLoS One*, *9*(4), e93957. https://doi.org/10.1371/journal.pone.0093957

Kanevskiy, M. (2003). *Cryogenetic structure of mountain slope deposits, northeast Russia*. Paper presented at the 8th International Conference on Permafrost.

Kanevskiy, M., Jorgenson, T., Shur, Y., O'Donnell, J. A., Harden, J. W., Zhuang, Q., & Fortier, D. (2014). Cryostratigraphy and permafrost evolution in the lacustrine lowlands of west-central Alaska. *Permafrost and Periglacial Processes*, *25*(1), 14–34. https://doi.org/10.1002/ppp.1800

Leewis, M.-C., Berlemont, R., Podgorski, D. C., Srinivas, A., Zito, P., Spencer, R. G. M., et al. (2020). Life at the frozen limit: Microbial carbon metabolism across a Late Pleistocene permafrost chronosequence. *Frontiers in Microbiology*, *25*, 1753. https://doi.org/10.3389/fmicb.2020.01753

Malmer, N., Albinsson, C., Svensson, B. M., & Wallén, B. (2003). Interferences between Sphagnum and vascular plants: Effects on plant community structure and peat formation. *Oikos*, *100*(3), 469–482. https://doi.org/10.1034/j.1600-0706.2003.12170.x

Manies, K. L., Fuller, C., & Jones, M. (2016). *Modeling peat ages using ^{7}Be Data to Account for Downwash of ^{210}Pb*. Paper presented at the American Geophysical Union Fall Meeting. Retrieved from https://ui.adsabs.harvard.edu/abs/2016AGUFM.B23C0597M

Manies, K. L., Fuller, C. C., Jones, M. C., Waldrop, M. P., & McGeehin, J. P. (2017). *Soil data for a thermokarst bog and the surrounding permafrost plateau forest, located at Bonanza Creek long term Ecological research site, interior Alaska (Open-File Report 2016-1173)*. U.S. Geological Survey.

Manies, K. L., Jones, M. C., Waldrop, M. P., Leewis, M.-C., Hoefke, K., Fuller, C., & Cornman, R. S. (2021). *Data supporting influence of permafrost type and site history on losses of permafrost carbon after thaw*. American Geophysical Union.

Manies, K. L., Waldrop, M., & Harden, J. (2020). Generalized models to estimate carbon and nitrogen stocks of organic soil horizons in interior Alaska. *Earth System Science Data*, *12*(3), 1745–1757. https://doi.org/10.5194/essd-12-1745-2020

Mason, O. K., & Begét, J. E. (1991). Late Holocene flood history of the Tanana River, Alaska, USA. *Arctic and Alpine Research*, *23*(4), 392–403. https://doi.org/10.2307/1551681

Miller, G. H., Geirsdóttir, Á., Zhong, Y., Larsen, D. J., Otto-Bliesner, B. L., Holland, M. M., et al. (2012). Abrupt onset of the Little Ice Age triggered by volcanism and sustained by sea-ice/ocean feedbacks. *Geophysical Research Letters*, *39*(2). https://doi.org/10.1029/2011gl050168

Natali, S. M., Watts, J. D., Rogers, B. M., Potter, S., Ludwig, S. M., Selbmann, A.-K., et al. (2019). Large loss of CO_2 in winter observed across the northern permafrost region. *Nature Climate Change*, *9*(12), 852–857. https://doi.org/10.1038/s41558-019-0644-0

Neumann, R. B., Moorberg, C. J., Lundquist, J. D., Turner, J. C., Waldrop, M. P., McFarland, J. W., et al. (2019). Warming effects of spring rainfall increase methane emissions from thawing permafrost. *Geophysical Research Letters*, *46*, 1393–1401. https://doi.org/10.1029/2018gl081274

Obu, J., Westermann, S., Bartsch, A., Berdnikov, N., Christiansen, H. H., Dashtseren, A., et al. (2019). Northern Hemisphere permafrost map based on TTOP modelling for 2000–2016 at 1 km^2 scale. *Earth-Science Reviews*, *193*, 299–316. https://doi.org/10.1016/j.earscirev.2019.04.023

O'Donnell, J. A., Jorgenson, M. T., Harden, J. W., McGuire, A. D., Kanevskiy, M., & Wickland, K. P. (2012). The effects of permafrost thaw on soil hydrologic, thermal, and carbon dynamics in an Alaskan peatland. *Ecosystems*, *15*, 213–229.

Olefeldt, D., Goswami, S., Grosse, G., Hayes, D., Hugelius, G., Kuhry, P., et al. (2016). Circumpolar distribution and carbon storage of thermokarst landscapes. *Nature Communications*, *7*, 13043. https://doi.org/10.1038/ncomms13043

Oliva, M., & Fritz, M. (2018). Permafrost degradation on a warmer Earth: Challenges and perspectives. *Current Opinion in Environmental Science & Health*, *5*, 14–18. https://doi.org/10.1016/j.coesh.2018.03.007

Parducci, L., Bennett, K. D., Ficetola, G. F., Alsos, I. G., Suyama, Y., Wood, J. R., & Pedersen, M. W. (2017). Ancient plant DNA in lake sediments. *New Phytologist*, *214*(3), 924–942. https://doi.org/10.1111/nph.14470

Parducci, L., Väliranta, M., Salonen, J. S., Ronkainen, T., Matetovici, I., Fontana, S. L., et al. (2015). Proxy comparison in ancient peat sediments: Pollen, macrofossil and plant DNA. *Philosophical Transactions of the Royal Society B: Biological Sciences*, *370*(1660), 20130382. https://doi.org/10.1098/rstb.2013.0382

Pella, E. (1990a). Elemental organic analysis. Part 1-Historical developments. *American Laboratory*, *22*(2), 116–125.

Pella, E. (1990b). Elemental organic analyzer. Part 2-State of the art. *American Laboratory*, *22*(12), 28–32.

R Core Team. (2017). *R: A language and environment for statistical computing*: R Foundation for Statistical Computing. Retrieved from https://www.R-project.org/

Rand, J., & Mellor, M. (1985). *Ice-coring augers for shallow depth sampling CRREL Report* (pp. 85–21). US Ice Drilling Program.

Rodenhizer, H., Ledman, J., Mauritz, M., Natali, S. M., Pegoraro, E., Plaza, C., et al. (2020). Carbon thaw rate doubles when accounting for subsidence in a permafrost warming experiment. *Journal of Geophysical Research: Biogeosciences*, *125*(6), e2019JG005528. https://doi.org/10.1029/2019jg005528

Sannel, A. B. K., & Kuhry, P. (2009). Holocene peat growth and decay dynamics in sub-arctic peat plateaus, west-central Canada. *Boreas: Boreas*, *38*(1), 13–24. https://doi.org/10.1111/j.1502-3885.2008.00048.x

Schädel, C., Schuur, E. A. G., Bracho, R., Elberling, B., Knoblauch, C., Lee, H., et al. (2014). Circumpolar assessment of permafrost C quality and its vulnerability over time using long-term incubation data. *Global Change Biology*, *20*(2), 641–652. https://doi.org/10.1111/gcb.12417

Schuur, E. A., McGuire, A. D., Schädel, C., Grosse, G., Harden, J. W., Hayes, D. J., et al. (2015). Climate change and the permafrost carbon feedback. *Nature*, *520*(7546), 171–179. https://doi.org/10.1038/nature14338

Shur, Y. L., & Jorgenson, M. T. (2007). Patterns of permafrost formation and degradation in relation to climate and ecosystems. *Permafrost and Periglacial Processes*, *18*(1), 7–19. https://doi.org/10.1002/ppp.582

Shur, Y. L., Jorgenson, M. T., & Kanevskiy, M. Z. (2011). Permafrost. In: In V. P. Singh, P. Singh, & U. K. Haritashya (Eds.), *Encyclopedia of snow, ice and glaciers* (pp. 841–848). Springer. https://doi.org/10.1007/978-90-481-2642-2_400

Soil Survey Staff. (1951). *Soil survey manual (Vol. Handbook No. 18)*. Agricultural Research Administration, United States Department of Agriculture.

Taberlet, P., Coissac, E., Pompanon, F., Gielly, L., Miquel, C., Valentini, A., et al. (2006). Power and limitations of the chloroplast *trn*L (UAA) intron for plant DNA barcoding. *Nucleic Acids Research*, *35*(3), e14.

Tanentzap, A. J., Burd, K., Kuhn, M., Estop-Aragonés, C., Tank, S. E., & Olefeldt, D. (2021). Aged soils contribute little to contemporary carbon cycling downstream of thawing permafrost peatlands. *Global Change Biology*, *27*(20), 5368–5382. https://doi.org/10.1111/gcb.15756

Thormann, M., Szumigalski, A., & Bayley, S. (1999). Aboveground peat and carbon accumulation potentials along a bog-fen-marsh wetland gradient in southern boreal Alberta, Canada. *Wetlands*, *19*(2), 305–317. https://doi.org/10.1007/bf03161761

Treat, C. C., & Jones, M. C. (2018). Near-surface permafrost aggradation in Northern Hemisphere peatlands shows regional and global trends during the past 6000 years. *The Holocene*, *28*(6), 998–1010. https://doi.org/10.1177/0959683617752858

Treat, C. C., Jones, M. C., Camill, P., Gallego-Sala, A., Garneau, M., Harden, J. W., et al. (2016). Effects of permafrost aggradation on peat properties as determined from a pan-Arctic synthesis of plant macrofossils. *Journal of Geophysical Research: Biogeosciences*, *121*(1), 78–94. https://doi.org/10.1002/2015jg003061

Treat, C. C., Wollheim, W. M., Varner, R. K., Grandy, A. S., Talbot, J., & Frolking, S. (2014). Temperature and peat type control CO_2 and CH_4 production in Alaskan permafrost peats. *Global Change Biology*, *20*(8), 2674–2686. https://doi.org/10.1111/gcb.12572

Turetsky, M. R., Kane, E. S., Harden, J. W., Ottmar, R. D., Manies, K. L., Hoy, E., & Kasichke, E. S. (2011). Recent acceleration of biomass burning and carbon losses in Alaskan forests and peatlands. *Nature Geosciences*, *4*, 27–31. https://doi.org/10.1038/ngeo1027

Turetsky, M. R., Manning, S. W., & Wieder, R. K. (2004). Dating recent peat deposits. *Wetlands*, *24*(2), 324–356. https://doi.org/10.1672/0277-5212(2004)024[0324:drpd]2.0.co;2

Vitt, D., Marsh, J., & Bovey, R. (1988). *Mosses, lichens and ferns of northwest North America*. Lone Pine Publishing.

Waldo, N. B., Hunt, B. K., Fadely, E. C., Moran, J. J., & Neumann, R. B. (2019). Plant root exudates increase methane emissions through direct and indirect pathways. *Biogeochemistry*, *145*(1), 213–234. https://doi.org/10.1007/s10533-019-00600-6

Waldrop, M. P., McFarland, J., Manies, K., Leewis, M. C., Blazewicz, S. J., Jones, M. C., et al. (2021). Carbon fluxes and microbial activities from boreal peatlands experiencing permafrost thaw. *Journal of Geochemical Research: Biogeosciences*, *126*(3), e2020JG005869. https://doi.org/10.1029/2020jg005869

Wolfe, S. A., & Morse, P. D. (2017). Lithalsa formation and Holocene lake-level recession, Great Slave Lowland, Northwest Territories. *Permafrost and Periglacial Processes*, *28*(3), 573–579. https://doi.org/10.1002/ppp.1901

Wolfe, S. A., Short, N. H., Morse, P. D., Schwarz, S. H., & Stevens, C. W. (2014). Evaluation of RADARSAT-2 DInSAR seasonal surface displacement in discontinuous Permafrost Terrain, Yellowknife, Northwest Territories, Canada. *Canadian Journal of Remote Sensing*, *40*(6), 406–422. https://doi.org/10.1080/07038992.2014.1012836

Xie, C.-F., & Lou, H.-X. (2009). Secondary metabolites in bryophytes: An ecological aspect. *Chemistry & Biodiversity*, *6*(3), 303–312. https://doi.org/10.1002/cbdv.200700450

Yu, Z. (2006). Holocene carbon accumulation of fen peatlands in boreal western Canada: A complex ecosystem response to climate variation and disturbance. *Ecosystems*, *9*(8), 1278–1288.

Zhang, T., Heginbottom, J., Barry, R., & Brown, J. (2000). Further statistics on the distribution of permafrost and ground ice in the Northern Hemisphere. *Polar Geography*, *24*, 126–131. https://doi.org/10.1080/10889370009377692

Zimmermann, H. H., Raschke, E., Epp, L. S., Stoof-Leichsenring, K. R., Schwamborn, G., Schirrmeister, L., et al. (2017). Sedimentary ancient DNA and pollen reveal the composition of plant organic matter in Late Quaternary permafrost sediments of the Buor Khaya Peninsula (North-Eastern Siberia). *Biogeosciences*, *14*(3), 575–596. https://doi.org/10.5194/bg-14-575-2017